Available online at www.sciencedirect.com

ScienceDirect

Procedia Engineering 213 (2018) 644–650

Procedia Engineering

www.elsevier.com/locate/procedia

7th International Conference on Fatigue Design, Fatigue Design 2017, 29-30 November 2017, Senlis, France

Local fatigue strength assessment of induction hardened components based on numerical manufacturing process simulation

M. Leitner[a]*, R. Aigner[a], D. Dobberke[b]

[a]*Montanuniversität Leoben, Chair of Mechanical Engineering, 8700 Leoben, Austria*
[b]*BMW Group, Research, New Technologies, Innovations, 85748 Garching, Germany*

Abstract

Induction hardening as common heat treatment process for highly-stressed automotive components significantly affects the surface layer properties leading to a compressive residual stress condition and a local hardening of the material. The beneficial effect of the post-treatment is generally well investigated and already implemented in industrial applicable guidelines by considering nominal fatigue strength enhancement factors. However, as the fatigue strength improvement essentially depends on the applied manufacturing process parameters, the resulting local material properties and the local load stress distribution, an elaborated numerical fatigue assessment procedure based on a manufacturing process simulation of a notched round specimen is presented in this paper. Thereby, a two-dimensional axi-symmetric model is set-up, whereby the inductive heating process is performed in COMSOL® and the subsequent quenching process in SYSWELD®. The resulting axial residual stress condition at the notch area of the specimen reveals a sound accordance to X-ray measurements. Finally, a local fatigue strength assessment based on the local strain approach is shown. Herein, manufacturing dependent residual stress states are considered as mean stresses on the basis of the damage parameter by Smith, Watson, and Topper. The estimated fatigue data points agree well to results of four-point bending fatigue tests, which basically prove the applicability of the presented fatigue design methodology.

Peer-review under responsibility of the scientific committee of the 7th International Conference on Fatigue Design.

Keywords: Fatigue strength; Induction hardening; Numerical simulation; Local fatigue assessment; Strain approach

* Corresponding author. Tel.: +43-3842-402-1463; fax: +43-3842-402-1402.
E-mail address: martin.leitner@unileoben.ac.at

1877-7058
Peer-review under responsibility of the scientific committee of the 7th International Conference on Fatigue Design.
10.1016/j.proeng.2018.02.060

1. Introduction

In general, induction hardening acts as common post-treatment process in industrial applications, such as gears [1], crankshafts [2], or railway axles [3]. Due to the surface-hardened layer, the wear resistance [4] as well as the fatigue performance [5] are usually increased. In case of the latter effect, benefit factors for the fatigue strength enhancement due to induction hardening are provided in fatigue design guidelines [6]. However, the resulting fatigue resistance of induction hardened components significantly depends on the applied process parameters and the resulting local material properties. In order to ensure a proper fatigue design, this paper demonstrates a method to estimate the local fatigue life on the basis of a numerical manufacturing process simulation [7]. The numerical simulation chain and the subsequent local fatigue assessment is applied on a representative specimen designed as notched round bar, see Fig. 1. The base material is a 50CrMo4 steel, which is common for induction hardened parts.

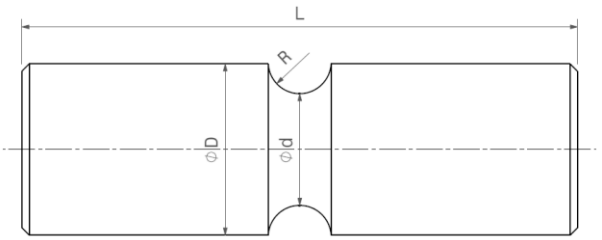

Fig. 1. Specimen geometry

Nomenclature

A	magnetic vector potential
B	magnetic flux density
b	fatigue strength exponent
C	heat capacity
c	fatigue ductility exponent
E	Young's modulus
J_e	external current density
K'	cyclic strength coefficient
N	number of load-cycles to fatigue failure
n'	cyclic strain hardening exponent
P_{WST}	Smith-Watson-Topper damage parameter
Q_{ind}	induced heat energy
ε_a	total strain amplitude
ε'_f	fatigue ductility coefficient
κ	electrical conductivity
λ	thermal conductivity
ω	angular frequency
ρ	material density
σ_a	stress amplitude
σ_m	mean stress
σ'_f	fatigue strength coefficient

2. Numerical simulation of manufacturing process

The numerical simulation chain is separated in two consecutive parts. At first, the inductive heating is performed utilizing the software package *COMSOL*® [8]. The resulting position and time dependent temperature field is subsequently transferred to the software package *SYSWELD*® [9], wherewith the simulation of the heat-treatment process is conducted. The presented methodology bases on a preliminary study given in [10].

2.1. Inductive heating process

Application studies for the utilized software tool are presented in [11, 12] and validations of the numerically evaluated results with experiments are shown in [13]. The principle of the incorporated electromagnetic simulation procedure is based on Maxwell's equations considering the magnetic vector potential by Equ. (1) [14].

$$\left(j\omega\kappa-\omega^2\varepsilon_0\varepsilon_r\right)A+\nabla\times\left(\mu_0^{-1}\mu_r^{-1}B\right)=J_e \;\; with \;\; B=\nabla\times A \tag{1}$$

Herein, j is the imaginary unit, ω is the angular frequency, κ is the electrical conductivity, ε_0 is the permittivity of vacuum, ε_r is the relative permittivity, A is the magnetic vector potential, μ_0 is the permeability in vacuum, B is the magnetic flux density, and J_e is external current density. The resulting induced heat energy is furthermore coupled with a thermal calculation of the heat transfer according to Equ. (2):

$$\rho C\frac{\partial T}{\partial t}=\nabla\cdot\left(\lambda\nabla T\right)+Q_{ind} \tag{2}$$

Where ρ is the material density, C is the heat capacity, λ is the thermal conductivity, and Q_{ind} is the induced heat energy. A representation of selected temperature dependent material properties for the investigated 50CrMo4 steel is provided in [16]. The numerical model for the inductive heating in *COMSOL*® is illustrated in Fig. 2. Thereby, a two-dimensional model is set-up due to the axi-symmetric specimen geometry. The specimen includes a relatively fine mesh in the surface region in order to accurately consider the skin-effect and subsequently surface hardening effects in this region of interest. The inductors consist of two separate coils exhibiting different frequencies of the electromagnetic field, which ensures a proper heating conditions as shown in [17] for induction hardened gears. For the numerical analysis in this study, the first coil features a medium frequency to facilitate global heating, and the second coil manifests a high frequency to intensify local heating within the surface layer of the specimen. As the two coils are moving along the axial axis of the specimen, a moving mesh is defined along this path. Finally, the ambient atmosphere is defined as air at room temperature and additionally meshed to incorporate interaction phenomena during the inductive heating process.

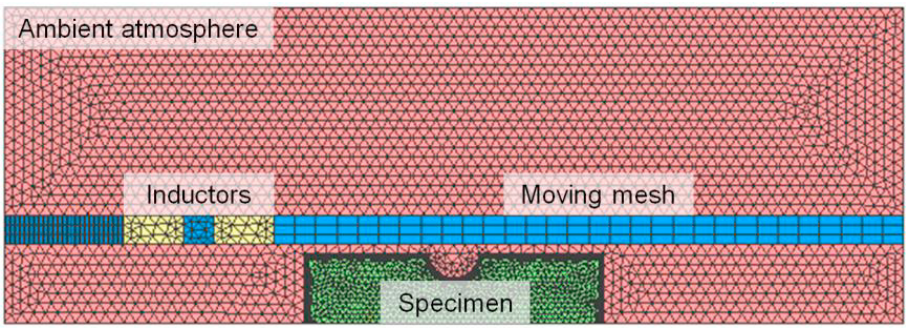

Fig. 2. Numerical model for inductive heating (according to [10])

Fig. 3 depicts the isothermal lines during different time steps of the inductive heating simulation. It can be clearly observed that the first coil leads to a global heating (see left picture) and the second coil ensures an intensified local heating within the surface layer of the specimen (see middle picture). This procedure leads to a suitable induction hardening especially in the area of the notch, which acts as main region of interest (see right picture).

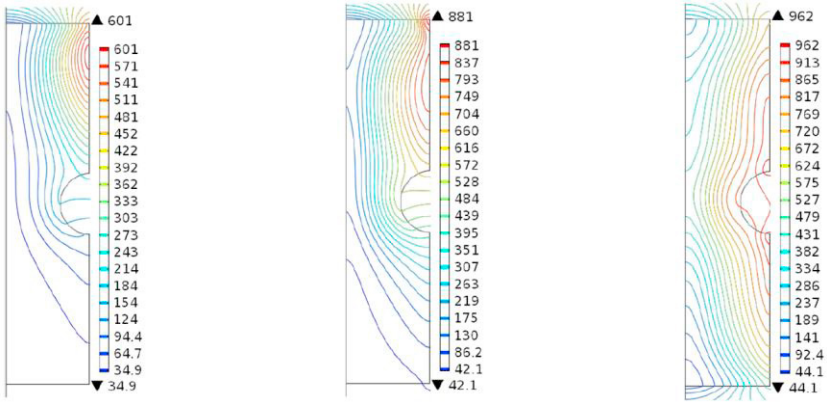

Fig. 3. Isothermal lines during inductive heating process in *COMSOL*® [10]

Subsequent to the inductive heating simulation, the time dependent nodal temperature values are transferred by a self developed routine to the software package *SYSWELD*® to perform the numerical analysis of the heat-treatment process. Further details in regard to the inductive heating simulation and the delevoped routine are provided in [10].

2.2. Heat-treatment process

Fig. 4 shows the heating process in *SYSWELD*® utilizing the imported time dependent nodal temperature field evaluated in *COMSOL*® for similar time steps as presented in Fig. 3. A comparison reveals that both temperature conditions agree well for each demonstrated time step, which basically validates the practicability of the presented methodology by transferring time dependent nodal temperature data between both software packages.

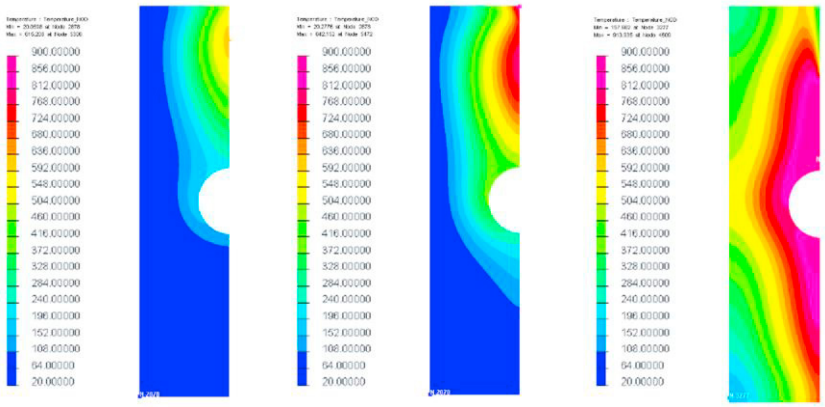

Fig. 4. Heating process in *SYSWELD*® [10]

After heating of the specimen, the quenching process is numerically simulated in *SYSWELD*®. The quenching is performed in two consecutive stages. At first, water spray cooling is performed directly after finishing of heating process. At second, air cooling is defined directly after finishing of the spray cooling process. The steps are defined in accordance to the experimental induction hardening process of the specimen. In [18] it is demonstrated that the cooling rate has a remarkable effect on the distortion and residual stress condition. Therefore, it is of utmost importance to properly model the cooling conditions within the heat-treatment simulation.

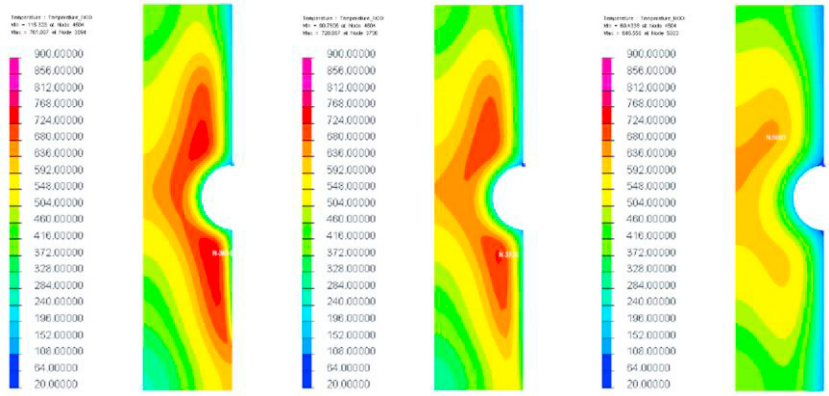

Fig. 5. Quenching process in *SYSWELD*® [10]

During quenching of the specimen, a coupled thermo-metallurgical-mechanical computation is executed in *SYSWELD*®. Detailed information regarding the incorporated material data is shown in [10]. The final axial residual stress condition at the notch root of the investigated specimen is illustrated in Fig. 6, whereby all values are normalized with the yield strength of the base material. A comparison of the X-ray measured and numerically computed axial residual stress values shows Tab. 1, which reveals that up to a measurement depth of 1 mm beneath the surface, a sound accordance is achieved. Hence, the presented numerical simulation chain is well capable to estimate the local residual stress condition of induction hardened 50CrMo4 steel notched components.

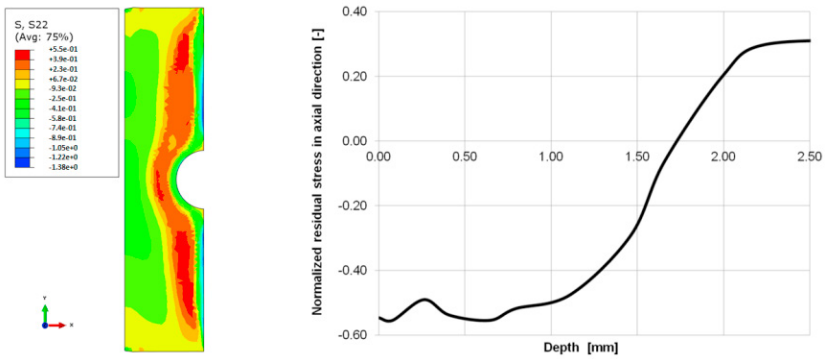

Fig. 6. Simulated axial residual stress condition after induction hardening process

Table 1. Comparison of normalized axial residual stress values

Evaluation procedure	Surface	Surface layer (1mm depth)	Core region (2mm depth)
X-ray residual stress measurement	-0.54	-0.52	Not available
Numerical manufacturing simulation	-0.55	-0.50	+0.20

3. Local fatigue strength assessment

Finally, a local fatigue strength assessment based on the common strain approach of the investigated notched round specimen is conducted. Thereby, the local total strain amplitude ε_a is determined by a cyclic stress-strain relationship introduced by Ramberg-Osgood [19] considering the linear-elastic stress amplitude σ_a, the Young's modulus E, the cyclic strength coefficient K', and the cyclic strain hardening exponent n', see Equ. (3).

$$\varepsilon_a = \frac{\sigma_a}{E} + \left(\frac{\sigma_a}{K'}\right)^{1/n'} \tag{3}$$

The numerically evaluated residual stress condition due to the induction hardening process is considered as mean stress value σ_m on the basis of the damage parameter P_{SWT} by Smith, Watson, and Topper [20], see Equ. (4).

$$P_{SWT} = \sqrt{(\sigma_a + \sigma_m)\varepsilon_a E} \tag{4}$$

The assessment of the number of load-cycles N until fatigue failure is performed applying the strain-life relationship by Manson [21], Coffin [22], and Basquin [23] involving the fatigue strength coefficient σ'_f, the fatigue strength exponent b, the fatigue ductility coefficient ε'_f, and the fatigue ductility exponent c, see Equ. (5).

$$P_{SWT} = \sqrt{\sigma'_f{}^2 (2N)^{2b} + \varepsilon'_f \sigma'_f E (2N)^{b+c}} \tag{5}$$

Low-cycle fatigue tests of through hardened small-scale specimens, which exhibit similar material properties as the induction hardened surface layer of the investigated notched round bar, are performed to evaluate the parameter data set for the hardened surface layer. The definition of the parameters for the core material is executed by employing the uniform material law by [24] using the extended version for high-strength steels given in [25]. The evaluation mostly depends on the local ultimate strength, which is estimated by local hardness measurements and a suggested hardness to quasi-static strength conversion procedure for steels provided in [26].

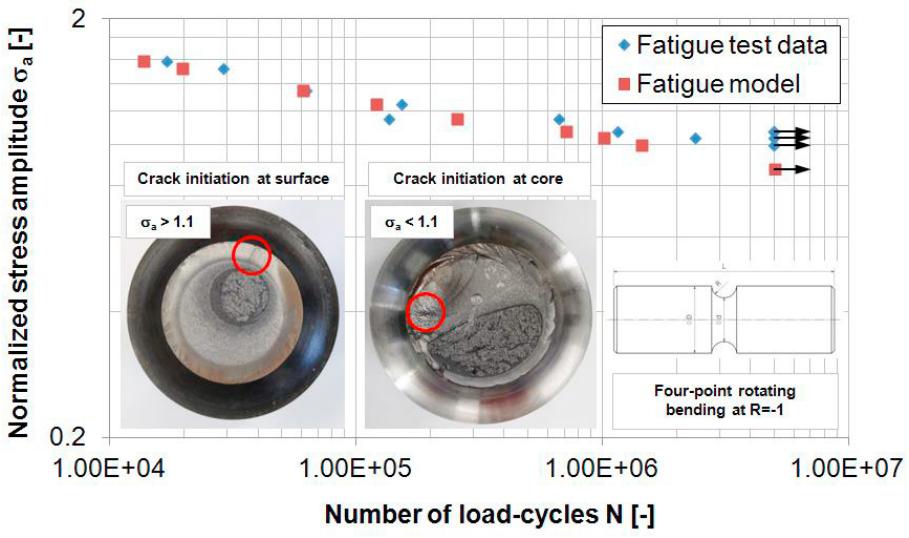

Fig. 7. Comparison of fatigue test data and estimation by local strain-based model

For comparison purpose, fatigue tests under four-point bending at a stress ratio of $R=-1$ are performed with the notched round specimens, see Fig. 7. The results are normalized to the minimal run-out load-level and indicate that in case of higher applied load stress amplitudes of $\sigma_a>1.1$, failure origin occurs at the surface of notch root. On the contrary, at minor stress amplitudes of $\sigma_a<1.1$, fatigue crack initiation takes place beneath the hardened surface layer within the core region. Therefore, it is utmost important to consider local manufacturing dependent residual stress, considered as mean stress, and material properties as well as local load stress and strain conditions in order to properly assess the failure location and fatigue life. The strain approach is applied at each corresponding load-level of the experiments and the results show a sound agreement with a minor conservative assessment.

4. Conclusions

This work presents a numerical manufacturing process simulation of the induction hardening and a subsequent local fatigue strength assessment. A notched round 50CrMo4 steel specimen is investigated as representative component. The two-dimensional simulation of the heat-treatment is performed utilizing the software packages *COMSOL*® and *SYSWELD*®. The numerically evaluated axial residual stress condition in the notch area reveals sound accordance to X-ray measurement results, which basically proves the practicability of the presented method. A final local fatigue assessment based on the local strain approach is demonstrated. Thereby, the residual stress state of the numerical manufacturing process simulation is considered as mean stress utilizing the damage parameter by Smith, Watson, and Topper. A comparison of the estimated and experimentally evaluated fatigue data points shows that the fatigue model, incorporating manufacturing dependent residual stress and material characteristics, is well applicable to estimate the fatigue strength of induction hardened steel components.

References

[1] V. Rudnev, D. Loveless, R. Cook, M. Back, Induction Hardening of Gears: a Review, Heat Treatment of Metals 4 (2003) 97-103.
[2] F. Garcia, Crankshaft Fillet Hardening: Challenges and Prospects, Industrial Heating (2014) 47-48.
[3] R. Fajkos, R. Zima, B. Strnadel, Fatigue limit of induction hardened railway axles, Fatigue Fract. Eng. Mater. Struct. 38 (2015) 1255-1264.
[4] M. Sofer, R. Fajkos, R. Halama, Influence of induction hardening on wear resistance in case of rolling contact, J. Mech. Eng. 66 (2016) 17-26.
[5] L. Bertini, V. Fontanari, Fatigue behaviour of induction hardened notched components, Int. J. Fat. 21 (1999) 611-617.
[6] FKM-Guideline: Analytical Strength Assessment of Components in Mechanical Engineering, 6th revised edition, VDMA, Frankfurt, 2012.
[7] F. Cajner, B. Smoljan, D. Landek, Computer simulation of induction hardening, J. Mat. Proc. Techn. 157-158 (2004) 55-60.
[8] R.W. Pryor, Multiphysics modeling using Comsol®, Jones and Bartlett Publishers, 2011.
[9] D. Pont, T. Guichard, Sysweld®: Welding and heat treatment modelling tools, Comp. Mech. (1995) 248-253.
[10] R. Aigner, Development of a numerical simulation chain for induction hardened boundary layers, Master thesis, Montanuniv. Leoben, 2016
[11] D. Istardi, A. Triwinarko, Induction Heating Process Design Using COMSOL® Multiphysics Software, Telkomnika 9 (2011) 327-334.
[12] M. Ocilka, D. Kovac, Simulation model of induction heating in COMSOL Multiphysics, Acta Elec. Inf. 15 (2015) 29-33.
[13] M. Kennedy, S. Akhtar, J. Bakken, R. Aune, Analytical and Experimental Validation of Electromagnetic Simulations Using COMSOL®, re Inductance, Induction Heating and Magnetic Fields, Proceedings of the 2011 COMSOL Conference, 2011.
[14] V. Rudnev, D. Loveless, R. Cook, M. Black, Handbook of induction heating, CRC Press, 2002.
[15] COMSOL Multiphysics®, Reference Manual Version 4.3b, 2013.
[16] J. Barglik, A. Smalcerz, R. Przylucki, I. Dolezel, 3D modeling of induction hardening of gear wheels, J. Comp. App. M. 270 (2014) 231-240.
[17] T. Petzold, D. Hömberg, D. Nadolski, A. Schulz, H. Stiele, Adaptive Finite Element Simulations of Multifrequency Induction Hardening in 3D, J. Heat Treatm. Mat. 70 (2015) 33-39.
[18] Z. Li, B. Ferguson, V. Nemkov, R. Goldstein, J. Jackowski, G. Fett, Effect of Quenching Rate on Distortion and Residual Stresses During Induction Hardening of a Full-Float Truck Axle Shaft, J. Mat. Eng. Perf. 23 (2014) 4170-4180.
[19] W. Ramberg, W.R. Osgood, Description of stress–strain curves by three parameters, Technical Note No. 902, National Advisory Committee for Aeronautics, Washington DC, 1943.
[20] K.N. Smith, P. Watson, T.H. Topper, A stress-strain function for the fatigue of materials, J. Mater. 5 (1970) 767-778.
[21] S.S. Manson, Fatigue: a complex subject – some simple approximation, Exp. Mech. 5 (1965) 193-226.
[22] L.F. Coffin, A study of the effect of cyclic thermal stresses on a ductile metal, Trans. ASME 76 (1954) 931-950.
[23] O.H. Basquin, The exponential law of endurance tests, Am. Soc. Test. Mater. Proc. 10 (1910) 625-630.
[24] A. Bäumel, T. Seeger, Material data for cyclic loading, Mater. Sci. Monogr. 61 (1990), Amsterdam: Elsevier Science Publishers.
[25] S. Korkmaz, Extension of the Uniform Material Law for High Strength Steels, Master thesis, Bauhaus University, 2008.
[26] E. Pavlina, C. Van Tyne, Correlation of Yield Strength and Tensile Strength with Hardness for Steels, J. Mat. Eng. Perf. 17 (2008) 888-893.